

Protective effects of PAMAM dendrimers against ANIT-induced cholestatic liver injury in mice

Chuang Zhang

Second Hospital of Hebei Medical University

Xuelai Liu

Capital Institute of Pediatrics Affiliated Children Hospital

Weirui Ren

Hebei Medical University Third Affiliated Hospital

Shaojie Liu

Hebei University of Science and Technology

Xiangjian Zhang

Second Hospital of Hebei Medical University

Desheng Yang

Hebei University of Science and Technology

Suolin Li (✉ 1550708140@qq.com)

Hebei Medical University second Affiliated Hospital

Research

Keywords: Cholestatic liver disease, PAMAM dendrimers, Inflammation, PPAR- γ , PI3K/AKT/mTOR

Posted Date: March 10th, 2020

DOI: <https://doi.org/10.21203/rs.3.rs-16550/v1>

License:   This work is licensed under a Creative Commons Attribution 4.0 International License.

[Read Full License](#)

Abstract

Background:Cholestatic liver disease (CLD) is a common disease of infancy, threatening infants' health seriously. However, there is no effective drug to treat this disease.It is urgently to develop a new drug to overcome it. Polyamide-amine (PAMAM) dendrimer is a hyperbranched nano polymer, which has been found that has an anti-inflammatory effect recently. For this study, we aim to explore the protective effect and mechanism of PAMAM on CLD.

Methods:In this study, a mouse model of cholestatic liver injury was created using ANIT,and TNF- α was utilized to stimulate human hepatocytes to investigate the protective effect and mechanism of 4.5th generation carboxyl-terminated PAMAM dendrimers (G4.5-COOH) in vivo and in vitro.Liver serum biochemistry, inflammatory, oxidative stress(OxS), endoplasmic reticulum(ER) stress and apoptosis indicators were determined.In addition, the effects of G4.5-COOH on PPAR- γ and PI3K/AKT/mTOR signaling pathway were studied. Data were analyzed by using one-way ANOVA.

Results:We find the G4.5-COOH may inhibit TNF- α to damage hepatocytes and ameliorate the cholestatic liver injury. We also find that the protective effect of G4.5-COOH might be due to inhibition of P-Akt/P-mTOR expression by a mechanism that might be partly dependent on up-regulated functional expression of PPAR- γ .

Conclusions:G4.5-COOH PAMAM dendrimer has a protective effect on CLD.

Background

CLD is the primary cause of consultation and hospitalization in infantile liver diseases, and it is also one of the important causes of infantile mortality or disability.[1, 2] Due to the obstruction of bile discharge, the accumulation of massive bile in hepatocytes leads to inflammation, OxS, apoptosis and fibrosis. Without effective treatment, it can eventually cause liver cirrhosis. [3]ANIT is a toxic reagent for the bile duct. Single-dose oral administration can induce acute biliary inflammation, leading to bile duct obstruction and producing intrahepatic cholestasis, which is similar to the pathological characteristics of human CLD and rat bile duct ligation model. [4]Therefore, it is an ideal model for the study on CLD.

PAMAM dendrimers are hyperbranched nanopolymers with diamine (usually ethylenediamine) as the core radiating from the center. They have well-defined controllable spherical structure and nanoscale.[5]Their internal cavity and high-density surface groups can increase the solubility and bioavailability of drugs through physical encapsulation, electrostatic interaction and covalent binding of drugs, genes, etc. They have been widely used in biomedical fields such as drug delivery, gene therapy, medical imaging and diagnosis, which are one of the most promising nanocarriers.[6–8]Recent studies have found that PAMAM itself has some biological activities and functions. For example, Chauhan et al. unexpectedly discovered that unmodified naked PAMAM with simple surface groups (such as -NH₂, -OH, etc.) had unexpected anti-inflammatory properties.[9]Yin et al. revealed that anionic and neutral PAMAM

dendrimers had protective effects on acute pancreatitis in mice, and their anti-inflammatory mechanism was related to the inhibition of nuclear translocation of NF- κ B in macrophages[10].

Cholestatic liver injury induces the accumulation of inflammatory cells and the secretion of proinflammatory cytokines. It has been proved that cholestatic liver injury is related to the re-emergence of inflammatory factors such as TNF- α , IL-6 and IL-1 β . [11, 12] Inflammatory cytokines are essential for inflammation, hepatocyte death, subsequent regeneration and hepatic fibrosis during the process of cholestatic liver injury.[3] Bile acids have been reported to contribute to the synthesis and excretion of IL-1 β and TNF- α . [13] PAMAM has an anti-inflammatory effect. It has been confirmed that G4.5-COOH has a certain therapeutic effect on a mouse model of pancreatitis. What about its effect on the liver? At present, the effect of PAMAM on the liver has not been reported. Therefore, we consider whether PAMAM can be applied to the prevention and treatment of liver diseases.

Materials And Methods

Synthesis of G4.5-COOH PAMAM Dendrimers

The G4.5-COOH was synthesized as described earlier with minor modification[14, 15]. The G4.5-COOH was synthesized as follows: The PAMAM dendrimers were synthesized by two steps at 25 °C according to a classical method. After vacuum rotation evaporation and G4.5-COOCH₃ were eventually obtained. In order to prepare G4.5-COOH, a certain volume of G4.5 PAMAM aqueous solution was placed in a round bottom flask, then 0.2M HCl solution was added dropwise to adjust the pH of solution to 1–2 and react at room temperature for 72 h. The synthesized dendrimers of G4.5-COOH were purified by membrane dialysis to remove a portion of the trailing generation defect structures.

Mice and Treatments

Healthy adult male Balb/C mice were supplied by the Experimental Animal Center of Hebei Medical University (Certificate no.:1708105,China). Mice were housed in a hygienic environment with a constant room temperature, and they had free access to food and water. All animals were acclimatized for 2 weeks prior to experiment.

Mice were divided into four groups with six mice per group. Mice in control group was treated intravenously (i.v.) with normal saline (NS) q.o.d. for 2 weeks, and on the twelfth day were given the vehicle(olive oil) alone. ANIT group was treated with normal saline (NS) q.o.d. for 2 weeks and severally administrated with 100 mg/kg ANIT(TCI,Japan)(dissolved in olive oil)on the twelfth day.-COOH + ANIT group was treated intravenously (i.v.) with G4.5-COOH at a dose of 50 mg/kg q.o.d. for 14 days according to a regimen published by literature[10] and severally administrated with 100 mg/kg ANIT(dissolved in olive oil)on the twelfth day; GW9662+COOH + ANIT group was treated with GW9662(ApexBio,USA)3 mg/kg[16] at 0.5 h before G4.5-COOH reatment,the rest of steps are the same as -COOH + ANIT group.

Cells and Treatments

Human hepatocyte cells (THLE) were kindly provided by department of Biochemistry from Hebei Medical University in China. Cells were cultured in RPMI-1640 medium (Gibco, USA) with 10% fetal bovine serum (FBS, Gibco, USA) and 1% (v/v) Penicillin-streptomycin solution (Gibco, USA) at 37°C and 5% CO₂.

The cells were divided into four groups: (1) Control group; (2) TNF- α group:stimulated with TNF- α (10 ng/ml) [17]alone for 24 hours; (3) -COOH + TNF- α group :preincubation with G4.5-COOH (7 μ M) for 4 h before TNF- α stimulation; (4) GW9662 +COOH + TNF- α group : GW9662 (10 μ M/ml) [18]was added for 0.5 h and then preincubation with G4.5-COOH (7 μ M) for 4 h before TNF- α stimulation.

Cell Viability Assay

THLE cells were seeded in 96-well plate at the density of 1×10^4 cells/well in the presence of G4.5-COOH at concentrations of 0-630 μ M for 24 h. CCK8 (Dojindo Laboratories,Japan)was added to cells and incubated for 4 h ,the viability of the cells was measured at 450 nm using a multifunctional microplate reader (SPARK 10M, TECAN, Switzerland).

Serum Biochemical Examination

Serum levels of TBiL, DBiL,TBA, ALT,AST and ALP were examined by LABOSPECT 008 AS automatic biochemistry analyzer(HITACHI,Japan).

Oxidative Stress Measurement

The assay method of SOD ,GSH and MDA levels in liver tissues and THLE cells was following the instructions of the kits provided by Suzhou Geruisi Biotechnology Co., Ltd (China).

Gene Expression Assay

Total RNA from liver tissues was extracted by utilizing TRIzol reagent(TIANGEN Biotech,Beijing), and first-strand cDNA was generated by a RT kit (TaKaRa Bio,Japan). Then,1 μ g of isolated RNA was reverse-transcribed into cDNA. The primers for proinflammatory cytokines were TNF- α ,(F)5'-CTC CTC ACC CAC ACC ATC AGC CGC A -3',(R)5'- ATA GAT GGG CTC ATA CCA GGG CTT G-3'; IL-6,(F)5'-AAA GAT GGC TGA AAA AGA TGG ATG-3',(R)5'-CAA ACT CCA AAA GAC CAG TGA TGA T-3';and IL-1 β ,(F)5'-CCA CCT CCA GGG ACA GGA TA-3',(R)5'-AACACG CAG GAC AGG TACAG-3'.PCR amplification and detection were conducted with an ABI7500 Real-Time Thermal Cycler(Applied Biosystems, Foster, CA, USA). The mRNA levels of these cytokines were normalized to those of 18 s.

HE and Immunohistochemistry

Fixed and embedded mouse liver tissues were sectioned and stained with hematoxylin-eosin (HE). To evaluate infiltration of macrophage and inflammatory cytokines in mouse liver tissues, F4/80 (Cell

Signaling Technology, USA) and TNF- α (Bioworld,China) immunohistological staining was performed on sections using a primary F4/80 (1:200) TNF- α (1:100) antibody and goat antirabbit IgG-HRP.

TUNEL

For determination of apoptosis in situ, colorimetric apoptosis detection was performed with the terminal deoxynucleotidyl transferase dUTP nick end labelling (TUNEL) reaction according to the manufacturer's instructions(KeyGEN,China).

Flow Cytometry

The percentage of apoptotic THLE cells was measured using a commercial kit (Absin, China). THLE cells were stained with FITC-labelled Annexin V (1 mg/mL) and propidium iodide (10 mg/mL) for 15 min. After gentle washes, patterns of apoptotic cells were measured using a FACSVerse (Becton-Dickinson, USA).

Western Blots

Tissues and cells were lysed with RIPA buffer (Solarbio,China) respectively. The concentration of total lysate was measured by using a BCA kit (Solarbio,China). A total of 30ug samples were separated on a 10% SDS-PAGE gel and transferred onto 0.4 mM PVDF membranes(MILLPORE,USA). The membranes were blocked with 5% BSA-PBST buffer for 1 h, followed by the incubation with primary anti-bodies overnight at 4°C and HRP-linked secondary antibodies (KPL,USA) for 2 h at RT. Bands were detected using enhanced chemiluminescence (ECL) prime reagent (Vazyme,China). Intensity of bands was assessed using Image-J software.

Statistics

The results are expressed as mean \pm SD. The statistical significance of the experimental data was analysed by one-way ANOVA. $P < 0.05$ was considered statistically significant.

Results

Characterization of G4.5-COOH PAMAM Dendrimers

The FTIR spectrum of G4.5-COOCH₃ and G4.5-COOH was shown in Fig. 1. Compared with G4.5-COOCH₃, G4.5-COOH have a strong absorption band around 3430.37 cm^{-1} , corresponding to the stretching vibration peak of the hydroxyl group in the carboxylic acid. A strong carbonyl O = C-O characteristic absorption peak appeared near 1737.61 cm^{-1} , meanwhile a strong absorption peak of -C-O- appeared near 1414.87 cm^{-1} , indicating the presence of carboxyl groups (Fig. 1).

G4.5-COOH Alleviated ANIT-induced Cholestatic Liver injury in Mice

After gavage administration with ANIT, the mice presented mental sluggishness, messy and dull hair, dementia and physical inactivity, decreased appetite, reduced drinking, and dark yellow urine opposed to

the normal group. The livers were dark red with white necrotic foci, the gallbladders were significantly enlarged with cholestasis, and the serum was dark and turbid. Report to ANIT group, -COOH + ANIT group showed significant improvement in spirit, hair, appetite and activity, the color of urine and liver was obviously lighter, the gallbladders were smaller and serum was clearer. However, after adding GW9662, the mice showed poorer spirit, hair, appetite and activity, darker urine, darker livers, larger gallbladders and more turbid serum than those in -COOH + ANIT group (Fig. 2).

Next, we detected the serum markers of liver functions including TBIL, DBIL, TBA, AST,ALT and ALP. Compared with control group, The levels of TBIL, DBIL, TBA, AST,ALT and ALP in ANIT group increased significantly ($P < 0.01$ or $P < 0.001$); Compared with ANIT group, the levels of TBIL, DBIL, TBA, AST,ALT and ALP in -COOH + ANIT group decreased significantly ($P < 0.01$ or $P < 0.001$); However, after adding GW9662, TBIL, DBIL, TBA, AST,ALT and ALP levels in GW9662 + -COOH + ANIT group were significantly higher than those in -COOH + ANIT group ($P < 0.01$ or $P < 0.001$) (Fig. 3).

G4.5-COOH Reduced Inflammation induced by ANIT treatment in Mice

The control group showed a normal portal triad comprising of the bile duct, hepatic artery and portal vein. In ANIT group, dilatation and hemorrhage of the portal vein, bile duct epithelial hyperplasia, bile duct stenosis and cholestasis were observed. Moreover, a large number of inflammatory cells infiltrated the portal area, with punctate and focal necrotic areas. In -COOH + ANIT group, the bile duct epithelium was slightly damaged and inflammatory cell infiltration was rare, almost returned to the conditions of the control group. In GW9662 + -COOH + ANIT group, bile duct epithelial hyperplasia, inflammatory cell infiltration and focal necrosis of the liver were increased (Fig. 4.A).

Immunohistochemical results demonstrated extensive macrophage infiltrated around the bile duct, vessels and in the necrotic lesions ($P < 0.001$). Compared with ANIT group, liver tissues from G4.5-COOH-treated mice demonstrated significant inhibition in macrophage and TNF- α infiltration (F4/80: $P < 0.001$, TNF- α : $P < 0.001$). While macrophages and TNF- α significantly increased in GW9662 + -COOH + ANIT group (F4/80: $P < 0.05$, TNF- α : $P < 0.001$) (Fig. 4.B-E).

The expression of inflammatory factors were significantly increased in ANIT-induced mice compared with normal control mice ($P < 0.001$). The expression of the pro-inflammatory cytokines TNF- α , IL-6 and IL-1 β was dramatically decreased in G4.5-COOH-treated mice ($P < 0.001$). However, in GW9662 + -COOH + ANIT group, the expression of inflammatory factors were higher than in -COOH + ANIT group ($P < 0.01$) (Fig. 4.F).

G4.5-COOH Decreased Cell Viability in A Concentration-Dependent Manner

In order to evaluate the cytotoxicity of G4.5-COOH and select appropriate concentration for further analysis, CCK8 was carried out. The results showed that G4.5-COOH decreased cell viability in a concentration-dependent manner. We chose the concentration of 7 μ M which had little effect on cell viability for following experiments (Fig. 5).

G4.5-COOH Reduced OxS in Cholestatic Liver Injury

Compared with the control group, SOD and GSH levels in liver tissues of ANIT group were significantly lower ($P \leq 0.001$) while MDA level was significantly higher ($P \leq 0.001$); Compared with ANIT group, the levels of SOD and GSH in -COOH + ANIT group increased significantly ($P \leq 0.001$), while the level of MDA decreased significantly ($P \leq 0.001$). However, after adding GW9662, SOD and GSH levels in GW9662 + -COOH + ANIT group were lower ($P < 0.01$ or $P < 0.001$) while MDA level was higher than those in the -COOH + ANIT group ($P < 0.05$) (Figure 6.A)

The same trend was observed in THLE cells. G4.5-COOH significantly reduced MDA level produced by TNF- α stimulation ($P \leq 0.001$) and increased SOD and GSH levels ($P < 0.01$ or $P < 0.001$). However, this effect was weakened by GW9662 ($P < 0.05$ or $P < 0.01$) (Figure 6.B).

G4.5-COOH Reduced ER Stress in Cholestatic Liver Injury

The expressions of CHOP and GRP78 proteins in liver tissues of ANIT group were significantly higher than those of control group (CHOP: $P \leq 0.01$, GRP78: $P \leq 0.001$). Compared with the ANIT group, CHOP and GRP78 protein expressions in -COOH + ANIT group decreased obviously (CHOP: $P \leq 0.05$, GRP78: $P \leq 0.01$). However, after adding GW9662, CHOP and GRP78 protein expressions in the GW9662 + -COOH + ANIT group were higher than those in -COOH + ANIT group ($P < 0.05$) (Fig. 7.A).

The same trend was observed in THLE cells. G4.5-COOH decreased CHOP and GRP78 protein expressions stimulated by TNF- α (CHOP: $P \leq 0.05$, GRP78: $P \leq 0.01$), but this effect was weakened by GW9662 ($P < 0.01$) (Fig. 7.B).

G4.5-COOH Reduced Liver Apoptosis in Cholestatic Liver Injury

The TUNEL staining and Bax/Bcl-2 protein results showed that compared with control group, the apoptosis rate was increased in ANIT group and reduced in -COOH + ANIT group ($P < 0.05$), indicating that G4.5-COOH inhibited liver cell apoptosis. However, after adding GW9662, the apoptosis rate was raised again ($P < 0.05$), indicating that GW9662 can antagonize the action of G4.5-COOH (Fig. 8.A-C).

Furthermore, THLE cells were incubated with Annexin V and propidium iodide (PI) dye and detected by a flow cytometer. The Flow Cytometry and Bax/Bcl-2 protein results showed that the apoptosis rate was significantly increased after interfering with TNF- α ($P < 0.05$), while G4.5-COOH reduced the rate of apoptosis and GW9662 increased the rate of apoptosis again ($P < 0.05$). These results indicated that G4.5-COOH could inhibit THLE cell apoptosis which induced by TNF- α (Fig. 8.D-F).

G4.5-COOH increased PPAR- γ expression through inhibiting PI3K/ Akt/mTOR signaling pathway in Cholestatic Liver Injury

Next, we ought to investigate whether PI3K/Akt/mTOR signaling pathway was involved in the increase PPAR- γ induced by G4.5-COOH. The protein levels of PPAR- γ was down-regulated and p-Akt, p-mTOR were

unregulated when exposing to ANIT or TNF- α ($P < 0.05$), and G4.5-COOH treatment further unregulated PPAR- γ expression and down-regulated p-Akt, p-mTOR expressions compared with ANIT or TNF- α group ($P < 0.05$), while the protein levels of Akt and mTOR were not significantly different between groups ($P > 0.05$). To further clarify the result, PPAR- γ inhibitor GW9662 was administrated to the mice and cells. Compared with G4.5-COOH + ANIT group, GW9662 markedly decreased the protein levels of PPAR- γ ($P < 0.05$), demonstrating that the inhibitor was effective. However at the same time the phosphorylation of mTOR and Akt was up-regulated again ($P < 0.05$). (Fig. 9.A-D)

Discussion

The molecular mechanism underlying the early liver injury associated with cholestasis remains unclear. It is generally accepted that high-concentration bile acids in hepatocytes and blood caused by cholestasis can produce direct toxicity to hepatocytes and induce hepatocyte apoptosis [19, 20]. However, with the development of analysis and detection technology, the quantitative determination of various bile acid components in the vivo model of cholestasis demonstrated that the concentration of bile acids was obviously insufficient to reach the concentration level that could directly cause cytotoxicity in vitro experiments, indicating that cholestatic liver injury has other pathogenesis besides the toxicity of bile acids [21–23]. Therefore, researchers began to focus on the role of inflammation and immune response caused by cholestasis on liver injury [24, 25]. The literature reported that 24 h after bile duct ligation, a large number of inflammatory cells infiltrated around the injured liver tissue [26, 27]. Our study also showed the necrosis of diseased hepatocytes accompanied by inflammatory cell infiltration in mice 48 h after ANIT administration. When the liver is stimulated by external trauma or harmful substances, macrophages are firstly activated to play a role of immune defense for phagocytosis and remove the harmful substances to protect the liver. However, with the secretion of inflammatory factors, excessive or unsolvable inflammatory reaction is nearly always accompanied by a massive loss of hepatocytes, resulting in irreversible damage to the hepatic parenchyma [28, 29]. TNF- α is part of the most important inflammatory factors. Numerous studies have shown that TNF- α is closely linked to liver diseases. It is not only an essential mediator of the inflammatory reaction, but also directly damages hepatic parenchymal cells [30, 31]. Our results confirmed extensive macrophage infiltration around the bile ducts, vessels and necrotic areas, and significantly increased TNF- α secretion in mice with cholestasis. Further, it showed that G4.5-COOH effectively inhibited the above inflammatory response.

Recent studies have found that ER stress plays a major role in various liver diseases, and its mechanism may be related to ER stress-induced apoptosis, which is a new hotspot in medical research [32, 33]. ER stress plays an important role in the body's inflammatory response. The effects of ER stress and inflammation are not unilateral. Inflammatory factors can also activate ER stress. TNF- α , IL-1 β and IL-6 can induce ER stress in hepatocytes and activate the cAMP response element binding protein H(CREB), thus mediate an acute-phase response (APR) [34]. The mechanism may be related to inflammatory factors promoting calcium release and ROS aggregation in the ER, thus interfering with the correct folding of proteins and mitochondrial metabolic balance [35]. Xue X et al. reported that TNF- α induced ROS accumulation and cell death. TNF- α induced unfolded protein response (UPR) in a ROS-

dependent manner, resulting in ER stress[36].This takes into account the relationship among inflammation, OxS and ER stress.Our study is consistent with the above findings that TNF- α induced ER stress in hepatocytes, and ANIT-induced cholestasis not only caused inflammation and OxS, but also caused ER stress injury in the mice liver. We are equally surprised to discover that G4.5-COOH has some effect on inhibiting ER stress.

Under normal physiological homeostasis, there is a dynamic balance between the number of newborn cells and apoptosis cells. Once this balance is broken (a relative increase in proliferating cells or apoptosis cells), pathological damage will be induced. Inflammation, OxS and ER stress can result in apoptosis [37, 38]. Our study revealed that the liver of mice with cholestasis induced by ANIT gavage had extensive apoptosis and necrosis. In vitro studies also found that TNF- α could induce the apoptosis of hepatocytes, while G4.5-COOH effectively inhibited apoptosis in vivo and in vitro.

PPAR- γ is part of the receptors of the PPAR family, which is highly produced in various organs, such as the liver and adipose tissues.Research show that PPAR- γ exerts direct anti-inflammatory effects through suppression of NF- κ B down-regulates its downstream pro-inflammatory factors,such as TNF- α . [39, 40]It is under a protective effect on liver.[41] PPAR- γ agonists also can inhibit monocytes activation and inflammatory factors release.[42, 43] Numerous studies have shown Nrf-2 and PPAR- γ can mutually activate each other, they showed synergistic protection against liver injury. [44–46]Our studies revealed that G4.5-COOH enhanced the expression levels of PPAR- γ thereby protecting liver function. The PI3K/AKT/mTOR signaling pathway plays an essential role in multiple cellular processes. Latest Studies manifested that it can promote liver fibrosis by activating PI3K/AKT/mTOR signaling.[47, 48] However,the effect and relationship of PPAR- γ and PI3K/AKT/mTOR signaling pathway in Cholestatic Liver disease is not certain. Through our research we found cholestatic liver can significantly elevate the P-Akt/P-mTOR protein expression. G4.5-COOH suppressed ANIT-induced P-Akt P-mTOR protein expression via up-regulation of PPAR- γ . GW9662 specifically inhibited the expression of PPAR, which could reverse the inhibitory effect of G4.5-COOH on the expression of p-akt and p-mtor. The same results were achieved when TNF- α was used to stimulate hepatocyte in vitro.

Conclusions

G4.5-COOH PAMAM dendrimer has a certain therapeutic effect on cholestatic liver injury. It may inhibit TNF- α to damage hepatocytes through inhibition of PI3K/AKT/mTOR signaling pathway by a mechanism that might be partly dependent on up-regulated functional expression of PPAR- γ .

Declarations

Acknowledgements

We appreciate all the assistance from Hebei Key Laboratory of Vascular Homeostasis and Hebei Collaborative Innovation Center for Cardio-cerebrovascular Disease in favour of this research.

Authors' contributions

CZ XL and DY proposed and designed the scope of the project. CZ and WR wrote the manuscript. CZ DY and SL conducted the experiments. WR and XZ analyzed the results and generated the figures. WR and XL assisted the animal studies. SL and DY critically revised and commented on the manuscript. All the authors read and approved the final manuscript.

Funding

Not applicable.

Availability of data and materials

All data generated and analyzed during this research are included in this article.

Ethics approval and consent to participate

All animal experiments of this study were approved by the Institutional Animal Care and Use Committee of the Second Hospital of Hebei Medical University (permit No. HMUSHC-130318), which are in line with the American Association for Laboratory Animal Science (AALAS) guidelines.

Consent for publication

All the authors consent for publication.

Competing interests

The authors declare that they have no competing interests.

References

1. Feldman AG, Sokol RJJN: Neonatal Cholestasis. 2013, 14:61-167.
2. Bruyne RD, Biervliet SV, Velde SV, Winckel MV: Clinical practice: neonatal cholestasis. 2011, 170:279-284.
3. Li S, Wang R, Wu B, Wang Y, Pharmakologie YYJAfEPu: Salvianolic acid B protects against ANIT-induced cholestatic liver injury through regulating bile acid transporters and enzymes, and NF- κ B/I κ B and MAPK pathways. 2019, 392.
4. Lin S, Wang T-Y, Xu H-R, Zhang X-N, Wang Q, Liu R, Li Q, Bi K-S: A systemic combined nontargeted and targeted LC-MS based metabolomic strategy of plasma and liver on pathology exploration of alpha-naphthylisothiocyanate induced cholestatic liver injury in mice. *Journal of pharmaceutical and biomedical analysis* 2019, 171:180-192.
5. Esfand R, Today DATJDD: Poly(amidoamine) (PAMAM) dendrimers: from biomimicry to drug delivery and biomedical applications. 6:427-436.
6. Wang B, Zhang K, Wang J, Zhao R, Zhang Q, Kong X: Poly(amidoamine)-modified mesoporous silica nanoparticles as a mucoadhesive drug delivery system for potential bladder cancer therapy. *Colloids and surfaces B, Biointerfaces* 2020, 189:110832-110832.

7. Stojceski F, Grasso G, Pallante L, Danani A: Molecular and Coarse-Grained Modeling to Characterize and Optimize Dendrimer-Based Nanocarriers for Short Interfering RNA Delivery. *ACS omega* 2020, 5:2978-2986.
8. Yuka M, Syungo I, Yu K, Aoi S, Hirohiko I, Tetsuya M, Hisatsugu Y, Akio T, Sensors KTJ: Pharmacokinetics of Chiral Dendrimer-Triamine-Coordinated Gd-MRI Contrast Agents Evaluated by in Vivo MRI and Estimated by in Vitro QCM. 15:31973-31986.
9. Chauhan AS, Diwan PV, Jain NK, Tomalia DAJB: Unexpected In Vivo Anti-Inflammatory Activity Observed for Simple, Surface Functionalized Poly(amidoamine) Dendrimers. 10:1195-1202.
10. Tang Y, Han Y, Liu L, Shen W, Zhang H, Wang Y, Cui X, Wang Y, Liu G, Qi RJB: Protective Effects and Mechanisms of G5 PAMAM Dendrimers against Acute Pancreatitis Induced by Caerulein in Mice. 16:174-182.
11. Gäbele E, Froh M, Arteel GE, Uesugi T, Hellerbrand C, Schölmerich J, Brenner DA, Thurman RG, Rippe RA: TNFalpha is required for cholestasis-induced liver fibrosis in the mouse. 2009, 378:348-353.
12. Gowert NS, Klier M, Reich M, Reusswig F, Donner L, Keitel V, Häussinger D, Elvers M: Defective Platelet Activation and Bleeding Complications upon Cholestasis in Mice. *Cellular physiology and biochemistry : international journal of experimental cellular physiology, biochemistry, and pharmacology* 2017, 41:2133-2149.
13. Miyake JH, Wang S-L, Davis RAJJoBC: Bile Acid Induction of Cytokine Expression by Macrophages Correlates with Repression of Hepatic Cholesterol 7 α -Hydroxylase. 275:21805-21808.
14. Tomalia DA, Baker H, Dewald J, Hall M, Kallos G, Martin S, Roeck J, Ryder J, Smith PJPJ: A New Class of Polymers: Starburst-Dendritic Macromolecules. 1985, 34:117-132.
15. Efficient reduction of 4-nitrophenol catalyzed by 4-carbo-methoxypyrrolidone modified PAMAM dendrimer–silver nanocomposites %J Catalysis Science & Technology. 2019.
16. He J, Hong B, Bian M, Jin H, Chen J, Shao J, Zhang F, Zheng S: Docosahexaenoic acid inhibits hepatic stellate cell activation to attenuate liver fibrosis in a PPAR γ -dependent manner. *International immunopharmacology* 2019, 75:105816-105816.
17. Zhu W, Qiu Q, Luo H, Zhang F, Wu J, Zhu X, Liang M: High Glucose Exacerbates TNF- α -Induced Proliferative Inhibition in Human Periodontal Ligament Stem Cells through Upregulation and Activation of TNF Receptor 1. *Stem cells international* 2020, 2020:4910767-4910767.
18. Gao J, Cheng Y, Hao H, Yin Y, Xue J, Zhang Q, Li L, Liu J, Xie Z, Yu S, et al: Decitabine assists umbilical cord-derived mesenchymal stem cells in improving glucose homeostasis by modulating macrophage polarization in type 2 diabetic mice. *Stem cell research & therapy* 2019, 10:259-259.
19. J M, Oscar P, Gastroenterology BJWJo: Bile-acid-induced cell injury and protection.1677-1689.
20. Wenniger LMDB, Digestive UBJ, Gastroenterology LDOJotlSo, Liver tIAftSot: Bile salts and cholestasis. 42:409-418.
21. Zhang Y, Hong JY, Rockwell CE, Copple BL, Klaassen CDJLIOJotlAftSotL: Effect of bile duct ligation on bile acid composition in mouse serum and liver. 2011, 32:58-69.

22. Burkard I, Eckardstein Av, B KMRJJoC: Differentiated quantification of human bile acids in serum by high-performance liquid chromatography–tandem mass spectrometry. 826:147-159.
23. Jocelyn T, Andrzej Be, Patrick C, J. SR, Piotr M, Olivier B, One GMJP: Profiling Circulating and Urinary Bile Acids in Patients with Biliary Obstruction before and after Biliary Stenting. 6:e22094-.
24. Gujral JS, Farhood A, Bajt ML, Jaeschke HJH: Neutrophils aggravate acute liver injury during obstructive cholestasis in bile duct–ligated mice. 2003, 38:355-363.
25. Allen K, Jaeschke H, Copple BL: Bile Acids Induce Inflammatory Genes in Hepatocytes: A Novel Mechanism of Inflammation during Obstructive Cholestasis. 178:0-186.
26. Tian X, Zhao H, Guo ZJCmm: Effects of carvedilol on expression of TLR4 and its downstream signaling pathway in liver tissue of rats with cholestatic liver fibrosis. 2020.
27. Zhang K, Shi Z, Zhang M, Dong X, Zheng L, Li G, Han X, Yao Z, Han T, Hong WJCD, Disease: Silencing lncRNA Lfar1 alleviates the classical activation and pyoptosis of macrophage in hepatic fibrosis. 2020, 11:1-13.
28. Brenner C, Galluzzi L, Kepp O, Kroemer GJJoh: Decoding cell death signals in liver inflammation. 59:583-594.
29. Woolbright BL, Reports JHJCP: Mechanisms of Inflammatory Liver Injury and Drug-Induced Hepatotoxicity.
30. Schwabe RF, Brenner DA: Mechanisms of Liver Injury. I. TNF- α -induced liver injury: role of IKK, JNK, and ROS pathways. 2006, 290:G583.
31. Ding WX, Yin XMJJoc, medicine m: Dissection of the multiple mechanisms of TNF- α -induced apoptosis in liver injury. 2004, 8:445-454.
32. Dara L, Ji C, Kaplowitz NJH: The contribution of endoplasmic reticulum stress to liver diseases. 2011, 53.
33. Malhi H, Kaufman RJ: Endoplasmic reticulum stress in liver disease. 54:0-809.
34. Zhang K, Shen X, Wu J, Sakaki K, Saunders T, Rutkowski DT, Back SH, Kaufman RJ: Endoplasmic Reticulum Stress Activates Cleavage of CREBH to Induce a Systemic Inflammatory Response. 124:0-599.
35. Lin W, Harding HP, Ron D, Popko BJJoCB: Endoplasmic reticulum stress modulates the response of myelinating oligodendrocytes to the immune cytokine interferon-gamma. 2005, 169:603-612.
36. Xue X, Piao JH, Nakajima A, Sakon-Komazawa S, Nakano HJJJoBC: TNF α induces the unfolded protein response (UPR) in a ROS-dependent fashion, and the UPR counteracts ROS accumulation by TNF α . 2005.
37. W P, Z C, D L, Pharmacology JYJ: Protective Effect of Diphenhydramine against Traumatic Brain Injury in Rats via Modulation of Oxidative Stress and Inflammation. 2019, undefined:1-7.
38. L D, C J, Hepatology KNJ: The contribution of endoplasmic reticulum stress to liver diseases. 2011, 53:1752-1763.

39. Genolet R, Wahli W, Michalik LJC*D-I*, Allergy: PPARs as Drug Targets to Modulate Inflammatory Responses? 2004, 3:361-375.
40. Zhang Y-F, Zou X-L, Jun W, Yu X-Q, Yang XJI: Rosiglitazone, a peroxisome proliferator-activated receptor (PPAR)- γ agonist, attenuates inflammation via NF- κ B inhibition in lipopolysaccharide-induced peritonitis. 2015, 38:2105-2115.
41. Zhang Y, Cui Y, Wang X-L, Shang X, Qi Z-G, Xue J, Zhao X, Deng M, Xie M-LJC: PPAR α / γ agonists and antagonists differently affect hepatic lipid metabolism, oxidative stress and inflammatory cytokine production in steatohepatic rats. 2015, 75:127-135.
42. Kostadinova R, Wahli W, Michalik LJC*mc*: PPARs in diseases: control mechanisms of inflammation. 2005, 12:2995-3009.
43. Jiang C, Ting AT, Seed BJ*N*: PPAR- γ agonists inhibit production of monocyte inflammatory cytokines. 1998, 391:82-86.
44. Park EY, Cho IJ, Kim SGJ*CR*: Transactivation of the PPAR-responsive enhancer module in chemopreventive glutathione S-transferase gene by the peroxisome proliferator-activated receptor- γ and retinoid X receptor heterodimer. 2004, 64:3701-3713.
45. A Faine L, Rudnicki M, A Cesar F, L Heras B, Boscá L, S Souza E, Z Hernandez M, L Galdino S, CA Lima M, R Pitta IJ*Cmc*: Anti-inflammatory and antioxidant properties of a new arylidene-thiazolidinedione in macrophages. 2011, 18:3351-3360.
46. Cho H-Y, Gladwell W, Wang X, Chorley B, Bell D, Reddy SP, Kleeberger SRJ*Ajor*, medicine cc: Nrf2-regulated PPAR γ expression is critical to protection against acute lung injury in mice. 2010, 182:170-182.
47. Wang H, Liu Y, Wang D, Xu Y, Dong R, Yang Y, Lv Q, Chen X, Zhang ZJ*C*: The Upstream Pathway of mTOR-Mediated Autophagy in Liver Diseases. 2019, 8:1597.
48. Gore E, Bigaeva E, Oldenburger A, Kim YO, Rippmann JF, Schuppan D, Boersema M, Olinga PJB*p*: PI3K inhibition reduces murine and human liver fibrogenesis in precision-cut liver slices. 2019, 169:113633.

Figures

Figure 1.

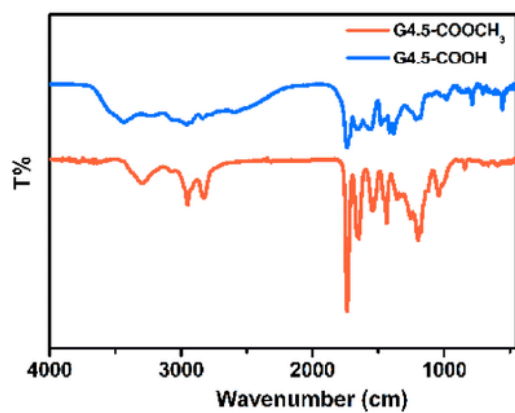


Figure 1

The FTIR spectrum of G4.5-COOCH₃ and G4.5-COOH PAMAM dendrimers.

Figure 2.

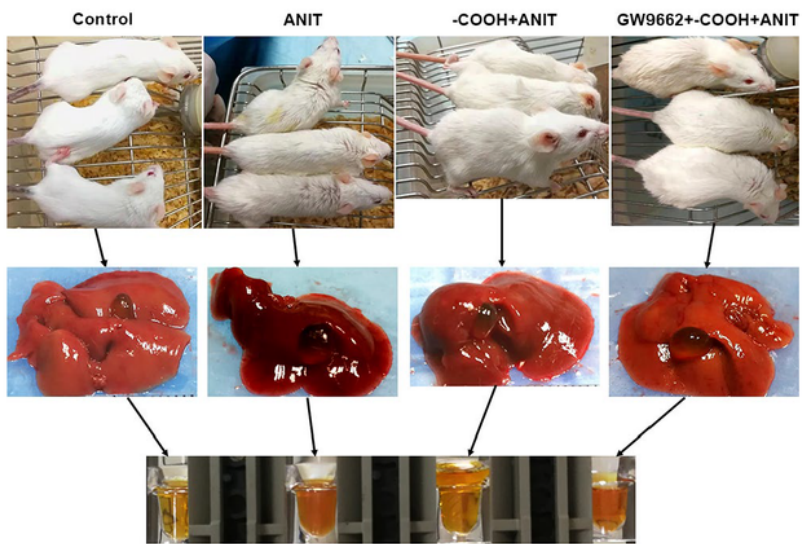


Figure 2

G4.5-COOH ameliorated the general conditions, liver and serum appearance of cholestatic mice.

Figure 3.

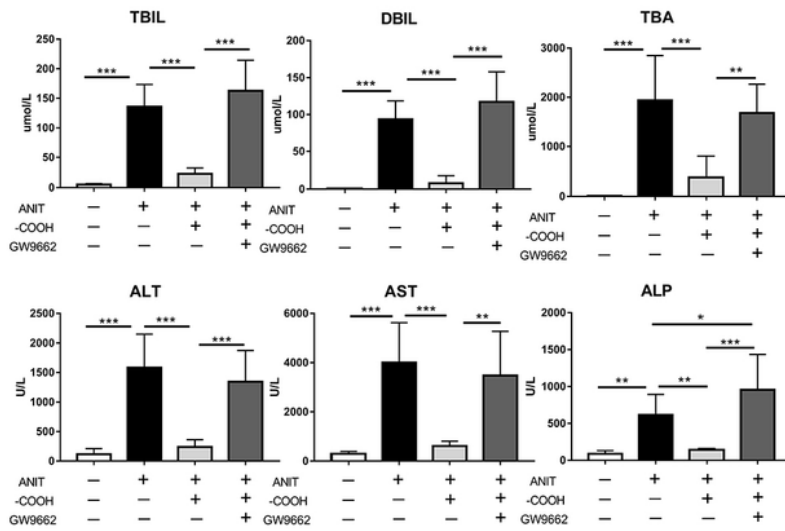


Figure 3

G4.5-COOH reduced liver functions serum markers. Values are the mean±SD for all groups; *P<0.05, **p<0.01 and ***P<0.001.

Figure 4.

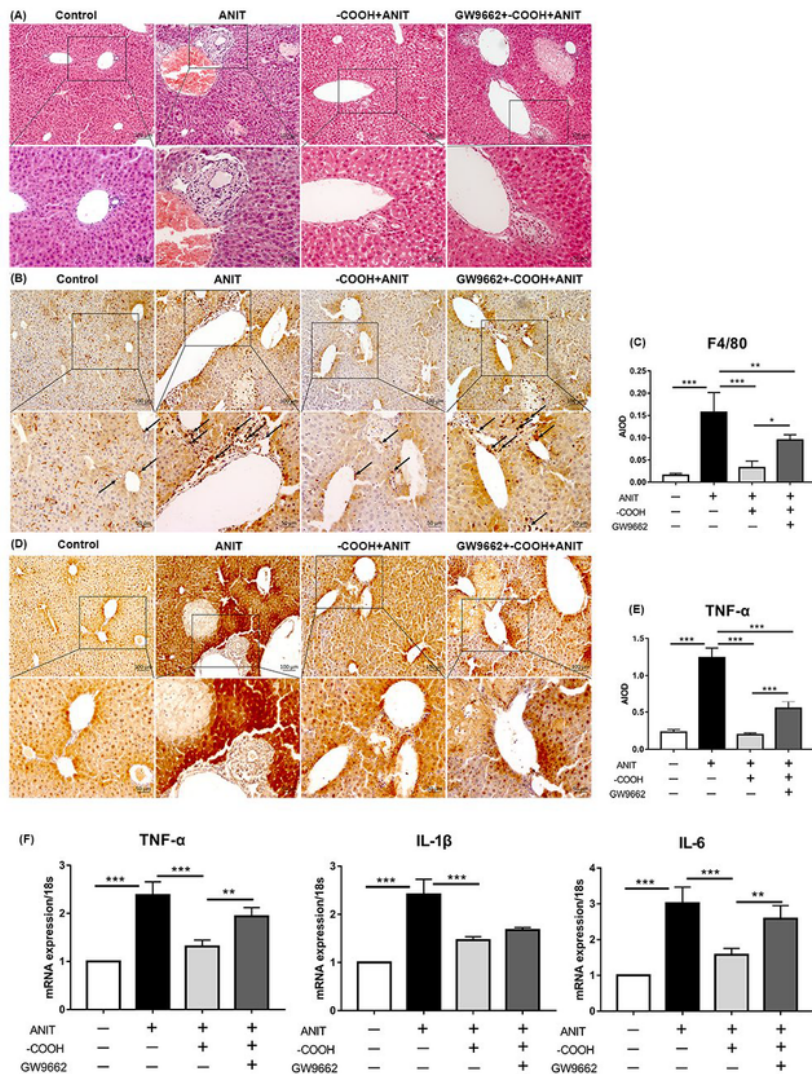


Figure 4

G4.5-COOH reduced inflammation induced by ANIT treatment in mice. (A) Histological changes in liver sections stained with H&E (100× or 200×); (B, C) Macrophage staining with F4/80 antibody (100× or 200×), black arrows indicate areas with positive macrophage staining; (D, E) TNF-α staining of mouse liver tissue (100× or 200×), TNF-α signals are stained in brown by DAB; (F) The mRNA expression of the pro-

inflammatory cytokines TNF- α , IL-6 and IL-1 β . Values are the mean \pm SD for all groups;*P<0.05, **p<0.01 and ***P<0.001.

Figure 5.

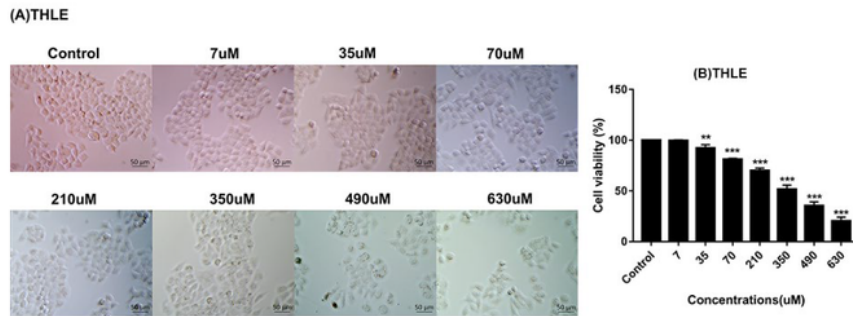


Figure 5

G4.5-COOH weakened cell viability in a concentration-dependent manner. The viability of (A,B) THLE cell lines treated with G4.5-COOH at a concentration range of 0–630 μ M is expressed as percentage of untreated cells(200 \times). Values are the mean \pm SD for all groups;*P<0.05, **p<0.01 and ***P<0.001.

Figure 6.

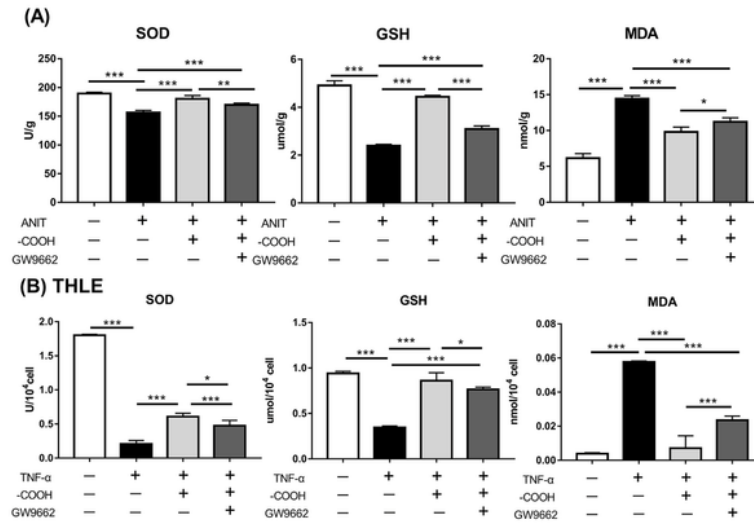


Figure 6

The protective potency of G4.5-COOH on some hepatic OxS parameters of cholestatic liver injury in vivo (A) and vitro (B). Values are the mean \pm SD for all groups; *P<0.05, **p<0.01 and ***P<0.001.

Figure 7.

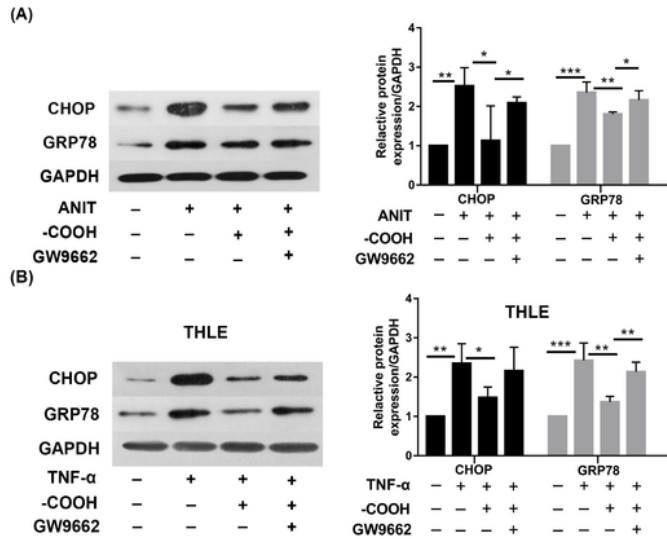


Figure 7

The protective potency of G4.5-COOH on some hepatic ER stress parameters of cholestatic liver injury in vivo (A) and vitro (B). Values are the mean±SD for all groups;*P<0.05, **p<0.01 and ***P<0.001.

Figure 8.

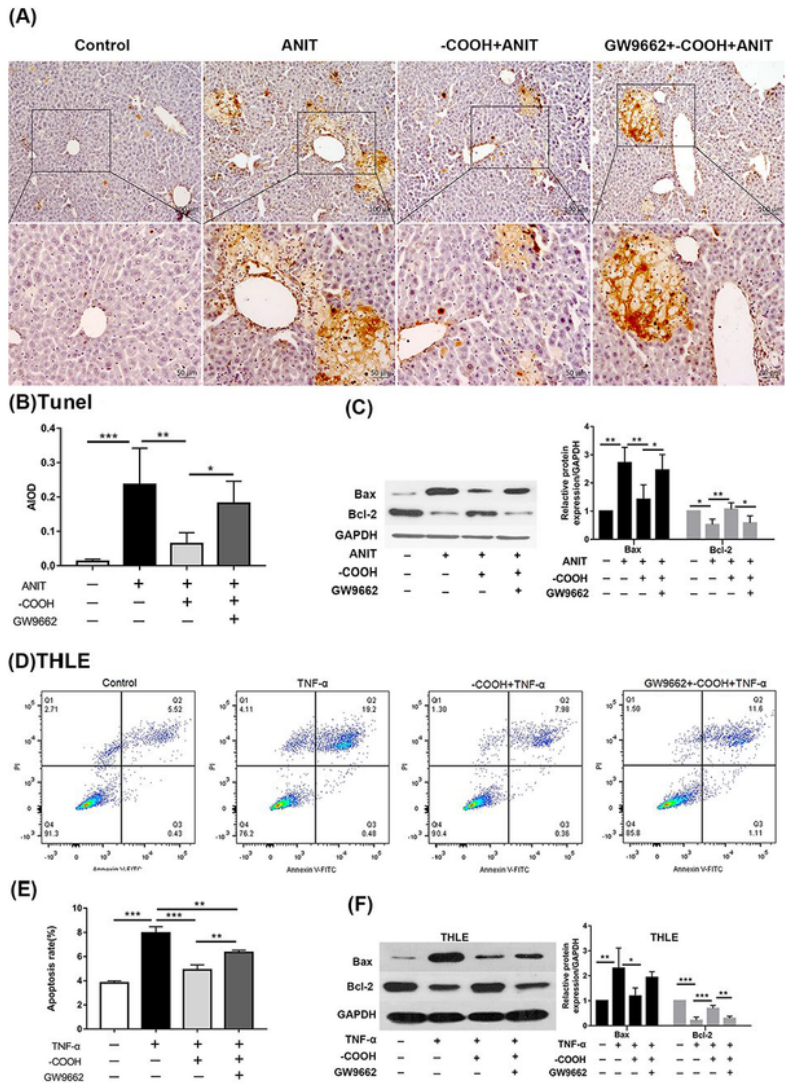


Figure 8

G4.5-COOH reduced liver apoptosis in cholestatic liver injury in vivo(A-C) and vitro(D-F). Values are the mean \pm SD for all groups; *P<0.05, **p<0.01 and ***p<0.001.

Figure 9.

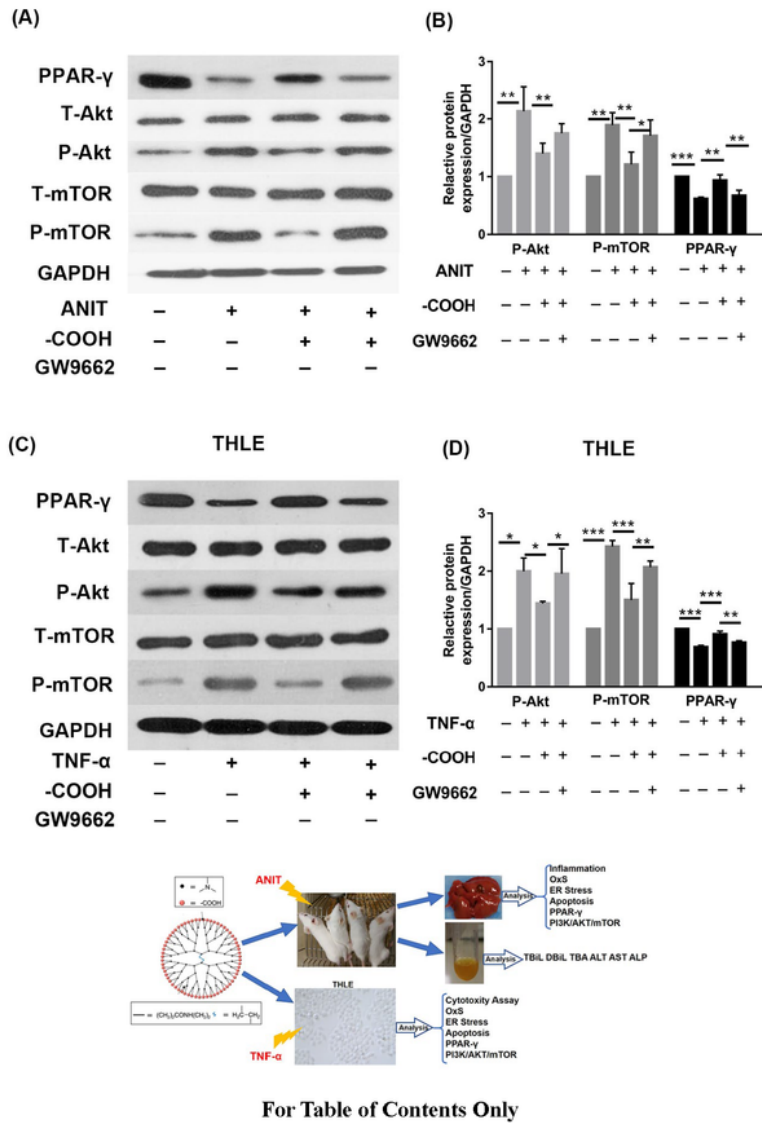


Figure 9

G4.5-COOH up-regulated the expression of PPAR-γ protein and down-regulated the expression of P-Akt and P-mTOR protein in cholestatic liver injury in vivo(A.B) and vitro(C.D). This effect was reversed by GW9662. Values are the mean±SD for all groups; *P<0.05, **p<0.01 and ***p<0.001.